Electric-field-induced optical rotation in the pretransitional isotropic region of chiral nematic liquid crystals

Jaskaran S. Kang and David A. Dunmur
Centre for Molecular Materials and Department of Chemistry, The University of Sheffield, Sheffield S3 7HF, United Kingdom
(Received 2 May 1994)

Measurements of the effect of an electric field on the pretransitional optical rotation in the isotropic phase of chiral nematic liquid crystal mixtures of (*S*)-4′(2-methylbutylphenyl)-4-*n*-decyloxybenzoate (CE6) and *n*-pentylcyanobiphenyl (CB5) are reported. Experiments were performed using an alternative technique for measuring circular birefringence in the presence of linear birefringence. The optical rotation results obtained fitted well with the existing theory of pretransitional optical activity. The critical temperature obtained from data fits varied as the square of the applied voltage as expected from the Landau–de Gennes theory. For some mixtures, the optical rotation changed sign on the application of a large electric field.

PACS number(s): 61.30.Gd, 78.20.Ek, 78.20.Jq, 78.66.−w

INTRODUCTION

On approaching the isotropic–liquid crystal phase transition by cooling, the characteristics of the ordered phase start appearing locally in the isotropic phase and become enhanced very near the transition point, giving rise to pretransitional phenomena. This increase of short range order over a correlation length near the phase transition results in a sharp increase of many properties (e.g., intensity of light scattering) as described by the Landau–de Gennes theory [1] of orientational order in the isotropic phase. Although the enhancement of optical rotation in the pretransitional isotropic region of chiral nematic liquid crystals was not anticipated [2], the first experimental evidence of pretransitional optical activity was reported by Cheng and Meyer [3,4]. Their observations can be understood in terms of growing local orientational order, resulting in increased intermolecular chiral interactions that enhance chiral fluctuations (i.e., the development of transient helicoidal structures) on approaching the transition point.

The director or local axis of orientational order in a chiral liquid crystal has a nonuniform spatial distribution. This can be represented in terms of five basic structural modes illustrated in Fig. 1 [5,19]. These modes are Fourier components having wave vector q and consist of an achiral nematiclike mode ($m=0$) in which the magnitude of the local order parameter varies, spiral conical modes ($m=\pm1$) in which the instantaneous local director is at 45° to the helix axis, and planar spiral modes ($m=\pm2$) for which the local director is at 90° to the helix axis. It has been shown [6] that to lowest order, only the conical spiral modes contribute directly to the pretransitional optical activity. However, for short pitch (i.e., ≤ 100 nm) systems in which blue phases [7,8] can exist, there can be a dominating contribution close to the phase transition from the planar spiral modes. In comparison with the conical spiral mode, the planar spiral mode makes an opposite contribution to the optical activity and has a higher divergence temperature so that a change in sign of the optical activity can occur close to the phase transition temperature. This has been observed experimentally [9] and a theoretical explanation has been provided by Filev [10]. In the chiral nematic phase a planar

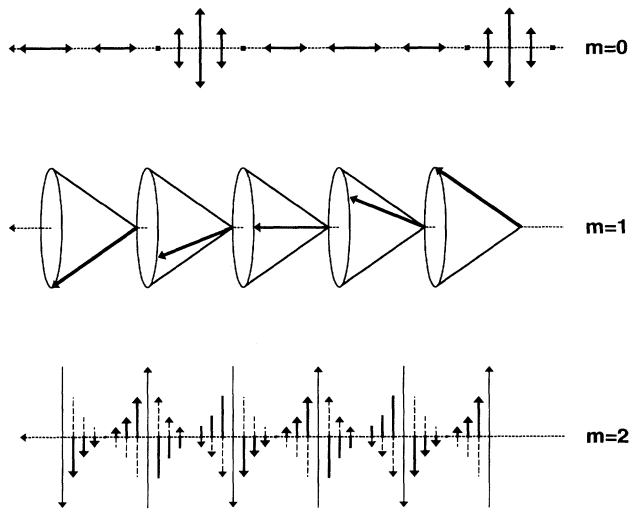

FIG. 1. Schematic representation of structural modes of the order parameter tensor for chiral liquid crystals. $m=0$: The tensor is represented by an ellipsoid of revolution about the arrow axes, and the ellipsoid alternates between horizontal and vertical, the double arrows representing the size and direction of the largest principal axis. $m=1$: The arrows represent the largest principal axis of the tensor, which rotates about and lies at 45° to the horizontal axis. $m=2$: The largest principal axis of the order parameter tensor rotates about, and is perpendicular to the horizontal axis. The arrows represent the projection of the principal axis on the plane of the diagram with the solid parts of the arrows above the plane of the diagram and the dashed parts below. Modes $m=-1$ and $m=-2$ are analogous to the $m=1$ and $m=2$ modes, respectively, but rotate in the opposite sense.

spiral mode having a particular wave vector q_0 is stabilized, resulting in the characteristic helicoidal structure of the phase. Light scattering measurements of the relative contributions of conical and planar spiral modes in the isotropic phase of highly chiral liquid crystals have been reported [11]. Similar measurements have been made by investigating the temperature dependence of the optical rotation [12–15], temperature dependence of the circular dichroism as a function of wavelength [16], and most recently, from optical rotation measurements as a function of the isothermal pressure [17,18]. A recent review [19] describes both theoretical and experimental aspects of optical activity and light scattering from chiral systems.

Chiral interactions in liquid crystals result in a variety of phases having helicoidal structures and strong optical activity. Materials designated as being strongly chiral show new phenomena such as antiferroelectric and ferrielectric smectic C phases, and for a few materials, the molecular twisting power is strong enough to distort the smectic layers to give filamental structures known as twist grain boundary phases [20]. The effect of molecular structure on these macroscopic manifestations of chirality is not known, but the study of chiral fluctuations on pretransitional behavior provides a probe of local interactions that are now directly related to molecular influences.

An optically isotropic liquid becomes birefringent when placed in a strong enough electric field. This is known as the Kerr electro-optic effect and results from field-induced molecular alignment. In the pretransitional isotropic region of nematics, electric-field-induced birefringence is strongly enhanced by local molecular order [21,22]. In this work, our aim has been to study chiral interactions by applying electric fields in the pretransitional isotropic region of chiral nematic liquid crystals. The increase in local orientational ordering induced by the field should result in an increase in the local chiral ordering, which would be manifested as an increase in optical activity. Hitherto, we are aware of only two reports of attempts to measure field-induced optical rotation. In one case, experiments using cholesteryl oleate [23] did not reveal any evidence of electric-field-induced optical rotation. We believe this may be due to the poor field aligning properties of that compound. Recently, Martinez-Miranda *et al.* [24] have reported results of field-induced optical activity in the pretransitional isotropic region of a smectic A material. They observed a small effect ($\sim 1°$) in a cell with path length of ~ 70 μm. In this work, we show convincingly, using much longer path lengths, that a large induced optical rotation is observed in the pretransitional isotropic region of certain chiral nematic liquid crystal mixtures that have sufficiently large dielectric anisotropy to obtain strong coupling to the electric field. We have studied this electro-chiral effect using a novel sensitive technique for determining optical rotation in the presence of linear birefringence.

THEORY

In general, plane polarized light travelling through an isotropic liquid of a chiral nematic material in a cell of thickness z will be rotated by angle ϕ:

$$\phi=\phi_0+\phi_{m=\pm1}+\phi_{m=\pm2}\ . \tag{1}$$

ϕ_0 is the intrinsic optical activity for a fluid which has no orientational order and is given by the expression [25]

$$\phi_0=\frac{16\pi^3 Nz}{\lambda^2 c_0}\beta\ , \tag{2}$$

where β is a molecular property known as the optical rotatory parameter, N is the number density, λ is the wavelength of light, and c_0 is the vacuum velocity of light. Optical activity due to chiral interactions arises from the conical spiral modes ($\phi_{m=\pm1}$) and the planar spiral modes ($\phi_{m=\pm2}$), although to lowest order only the $m=\pm1$ modes contribute. The remainder of this section will be devoted to a brief summary of the theory dealt with by several authors in detail, e.g., [9,26].

The local order in a liquid crystal can be represented in terms of the anisotropic part of the local dielectric tensor. For a cholesteric liquid crystal, the Landau–de Gennes free energy to second order can be written as [2,27,28]

$$F-F_0=\frac{1}{2}\int[a\varepsilon_{\alpha\beta}^2+b(\partial_\alpha\varepsilon_{\beta\gamma})^2+c\partial_\alpha\varepsilon_{\alpha\gamma}\partial_\beta\varepsilon_{\beta\gamma} -2\,de_{\alpha\beta\gamma}\varepsilon_{\alpha\delta}\partial_\gamma\varepsilon_{\beta\delta}]d^3r \tag{3}$$

where $\varepsilon_{\alpha\beta}$ is the dielectric tensor representing the local modes, $e_{\alpha\beta\gamma}$ is the Levi-Civita tensor, $a=a_0(T-T^*)$, the coefficients b, c, and d are considered to be temperature independent, and T^* is the second order phase transition temperature of the racemic mixture.

When the anisotropic part of the local dielectric tensor is expressed in terms of the five structural fluctuation modes discussed earlier, the free energy for terms up to second order can be written as [11,26]

$$F-F_0=\frac{1}{2}\sum_m\int d^3q\left\{a-m\,dq+\left[b+\frac{c}{6}(4-m^2)\right]q^2\right\}\times|\varepsilon_m(q)|^2\ , \tag{4}$$

where m is the label of the mode, q is the wave vector of the fluctuation, and $\varepsilon_m(q)$ is the amplitude of the mode. Each mode possesses a value of q which minimizes the free energy. In addition, using the expression for the coefficient a, the temperature at which the minimized free energy vanishes for each mode can be determined. At this temperature, the correlation length for each mode diverges:

$$T_0^*=T^*\ , \tag{5}$$

$$T_{\pm1}^*=T^*+\frac{bq_0^2}{4a_0(1+c/2b)}\ , \tag{6}$$

$$T_{\pm2}^*=T^*+\frac{bq_0^2}{a_0}\ , \tag{7}$$

where q_0 represents the chirality of the system (i.e., $q_0=d/b=4\pi/p$ and p is the pitch of the system).

To lowest order, the optical activity due to chiral interactions is enhanced only by the conical spiral mode

and diverges at T_1^*. Expressing the optical activity tensor in terms of $m=+1$ and $m=-1$ modes, applying the equipartition theorem to determine the amplitude of the fluctuation in each mode, and finally integrating over all wave vectors, the pretransitional optical activity contributed by $\phi_{m=\pm1}$ is given by

$$\phi_{m=\pm1}=\frac{k_B T k_0^2 q_0}{48\pi\bar{\varepsilon}\sqrt{a_0 b}}\left[1+\frac{c}{2b}\right]^{-3/2}\frac{1}{(T-T_1^*)^{1/2}}\ , \tag{8}$$

where k_B is Boltzmann's constant, k_0 is the wave vector of the light, and $\bar{\varepsilon}$ is the average dielectric constant.

If higher than second order terms are included in the free energy expansion (3), cross terms related to the conical and planar spiral modes occur, giving rise to an additional optical rotation. Although this is a higher order effect, fluctuations of the planar spiral mode may be quite large in the isotropic phase because this fluctuation diverges at T_2^* ($>T_1^*$). Since the optical rotation corresponding to the planar spiral mode is in the opposite sense from that due to the conical spiral mode, a peak occurs in the optical rotation just before the transition to the ordered phase. The optical activity due only to coupling of the conical and planar spiral modes is given by [10]

$$\phi_{m=\pm2}=-\frac{k_B T k_0^2 q_0}{48\pi\bar{\varepsilon}\sqrt{a_0 b}}\left[\frac{f(x,\tau)}{(T-T_2^*)^{1/2}}\right]\ , \tag{9}$$

where $f(x,\tau)$ is a function representing the mixing of the two modes, x is $q_0/2k_0$ (ratio of wavelength to pitch), and $\tau=T-T_2^*$. Thus the planar spiral modes can contribute to pretransitional optical activity through mode coupling. However, other mechanisms may allow the $m=\pm2$ modes to influence the pretransitional optical activity. Simplified expressions of (8) and (9) are used later for modeling the experimental results reported in this paper in which the temperature dependence of $f(x,\tau)$ is ignored.

EXPERIMENTAL DETAILS

Our polarimeter arrangement is shown in Fig. 2 and is based on the synchronous detection of a modulated optical signal with an EG&G, model 5210 lock-in amplifier. Instead of using a chopper [4] to produce the modulated signal, we used a Hinds International PEM-80 photoelastic modulator, which is a device for varying the polarization of the incoming light by a strain-induced birefringence. The light source from a 5-mW He-Ne (632.8 nm) laser was circularly polarized by a polarizer and quarter-wave plate combination. Circularly polarized light entering the modulator was converted to light that switched between linearly polarized states (at a 42-kHz rate) alternately polarized $+45°$ and $-45°$ to the transverse modulator axis. If the pass axis of the analyzer is at an azimuthal angle of θ, it can be shown using Mueller matrices that the transmitted light intensity I is given by

$$I=\tfrac{1}{2}I_0[1-\sin\delta_m\sin2(\phi+\theta)]\ , \tag{10}$$

where I_0 is the initial light intensity and δ_m is the modulator retardation. If $\delta_m=D\cos\omega t$, where D is a proportionality constant and ω is the modulation frequency, Eq. (10) can be rewritten as

$$I=\tfrac{1}{2}I_0\{1-\sin[D\cos\omega t]\sin2(\phi+\theta)\}\ . \tag{11}$$

On orienting the pass axis of the analyzer parallel to either of the modulator axes (i.e., $\theta=0°$), the frequency dependent term vanishes if the sample is optically inactive (i.e., $\phi=0°$). Hence no light modulated at 42 kHz appears at the photodiode. However, if the sample is optically active (i.e., $\phi>0°$), the right-hand side of Eq. (11) can be expanded as a series of Bessel functions:

$$\begin{aligned}I&=\tfrac{1}{2}I_0\left\{1-\left[2\sum_{k=0}^{\infty}(-1)^k J_{2k+1}(D)\cos(2k+1)\omega t\right]\sin2(\phi+\theta)\right\}\\&=\tfrac{1}{2}I_0\{1-[2J_1(D)\cos\omega t-2J_3(D)\cos3\omega t+\cdots]\sin2(\phi+\theta)\}\ .\end{aligned} \tag{12}$$

The fundamental frequency term was the source of the signal used for the synchronous detection of the optical rotation signal with the lock-in amplifier. To optimize the magnitude of the fundamental frequency signal, the peak-to-peak retardance of the modulator was set to 371 nm to maximize $J_1(D)$ [i.e., $D=1.841$ and $J_1(D)=0.582$]. Light transmitted from the analyzer was detected using a large area photodiode and the magnitude of the fundamental frequency signal was measured by the lock-in amplifier. The optical rotation was obtained directly with a precision of $\pm0.05°$ by recording the angle of rotation of the analyzer to null the fundamental frequency signal (i.e., $\theta=-\phi$).

Optical rotation measurements of chiral nematic liquid crystals of positive dielectric anisotropy were performed in 20-mm glass spectrophotometer cells. A specially made Teflon plug with vertical parallel plate electrodes of length ~16 mm and separated by ~2.7 mm was inserted into the glass cell. Voltages as large as 4 kV could be applied to these electrodes by a Brandenburg voltage supply. The cell was temperature controlled by circulating water from an electrically heated water bath to the cell holder, which had a temperature stability of $\pm0.05\,°C$. Each optical rotation measurement was made after waiting for ~5 min at constant temperature.

The linear birefringence of the sample should not

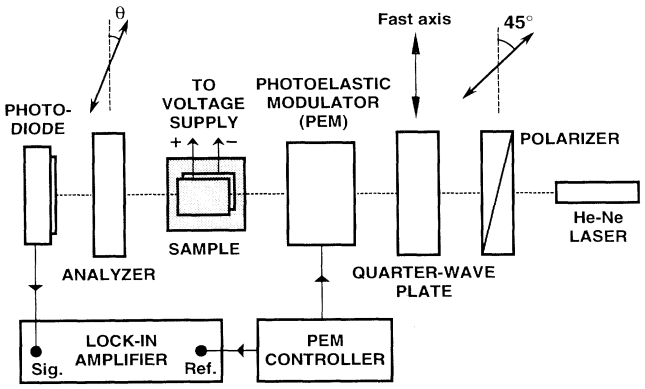

FIG. 2. Experimental setup for measuring the optical rotation of chiral systems as a function of temperature in the presence of an applied electric field; the laser beam was aligned so that it remained central between the parallel plate electrodes of the cell.

influence the optical rotation signal. This was checked theoretically by placing a linear retarder between the analyzer and sample in Fig. 2 and working through the Mueller matrices to determine the resulting transmitted light intensity expression:

$$I=\tfrac{1}{2}I_0[1-\cos 2\theta \sin 2\phi \sin\delta_m-(\cos\delta_L \cos 2\phi \sin\delta_m + \sin\delta_L \cos\delta_m)\sin 2\theta] , \tag{13}$$

where δ_L is the linear retardation. For small θ, (13) reduces to Eq. (10) and so for ideal optical elements, the presence of linear retardation does not contribute to the optical rotation, fundamental frequency signal.

The versatility of the setup in Fig. 2 is such that it can be configured with minor changes to measure the linear birefringence of a sample. To perform these measurements, it is necessary to remove the quarter-wave plate and cross the analyzer with the polarizer. If δ_s is the sample retardation, the light leaving the analyzer has intensity

$$I=\tfrac{1}{2}I_0[1-\cos(\delta_s+\delta_m)] . \tag{14}$$

By substituting $\delta_m = D\cos\omega t$ in (14) and expanding as a series in Bessel functions, the transmitted intensity is given by

$$I=\tfrac{1}{2}I_0\left[1-\left\{J_0(D)+2\sum_{k=1}^{\infty}(-1)^k J_{2k}(D)\cos(2\omega k t)\right\}\cos\delta_s+\left\{2\sum_{k=0}^{\infty}(-1)^k J_{2k+1}(D)\cos[(2k+1)\omega t]\right\}\sin\delta_s\right]$$
$$=\tfrac{1}{2}I_0[1-J_0(D)\cos\delta_s+2J_1(D)\cos(\omega t)\sin\delta_s-\cdots] . \tag{15}$$

The magnitude of the fundamental frequency signal is measured by the lock-in amplifier and corresponds to the linear birefringence of the sample.

RESULTS AND DISCUSSION

Initially, the chiral ester (*S*)-4′(2-methylbutylphenyl)-4-*n*-decyloxybenzoate (CE6) was selected for studying electric-field-induced phenomena. This material has a large intrinsic optical rotatory power (i.e., ~0.8°/mm) and a relatively low isotropic-chiral nematic phase transition temperature (i.e., 45.3 °C). The presence of the chiral nematic phase is important for enhancing field-induced effects in the pretransitional isotropic region. Furthermore, the racemate of CE6 was available so that control experiments could be performed to show that any induced optical activity was solely due to the chiral compound. Results on pure CE6 are shown in Fig. 3. The optical rotation diverges in the pretransitional isotropic region in a manner similar to that of other chiral nematic liquid crystals [3,27], but increases more sharply than that of chiral smectic liquid crystals [29,30]. However, no induced effect was observed on applying electric fields of ~1 kV/mm in either of the two configurations illustrated in Fig. 3. We believe that this is due to CE6 having very poor field aligning characteristics attributed to its very small dielectric anisotropy.

To increase the pretransitional order we selected a two component system of CE6 solute and *n*-pentylcyanobiphenyl (CB5) solvent. The latter component is archiral but has a large positive nematic dielectric anisotropy (i.e., $\Delta\varepsilon\sim+12$ at 25 °C), which results in a large pretransitional Kerr effect [21]. We found that a

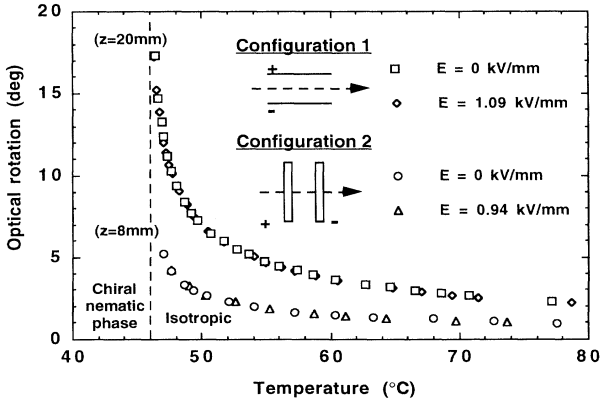

FIG. 3. The effect of an electric field on the optical rotation of pure CE6 for different configurations shown. In configuration 2, a cell with transparent electrodes was used. The arrows denote the direction of the laser light.

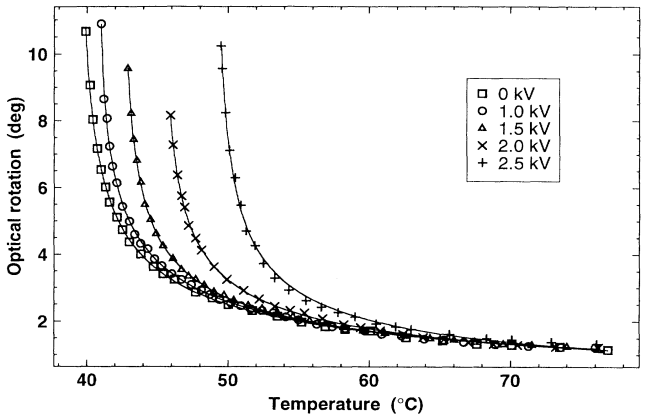

FIG. 4. Electric-field-induced optical rotation in the isotropic phase of mixture of composition 34% weight fraction (w/w) CE6–66% (w/w) CB5 using configuration 1 in Fig. 3. The solid lines are nonlinear least-squares fits using Eq. (16), i.e., $\phi=\phi_0+A/(T-T_1^*)^{1/2}$.

mixture of composition 34% (w/w) CE6 and 66% (w/w) CB5 was suitable to attain a compromise between a large degree of field-induced order resulting from CB5 and a large optical activity due to CE6. Results showing the existence of field-induced optical rotation on applying voltages of up to 2.5 kV to the mixture are presented in Fig. 4. In the pretransitional temperature region, the effect of the induced optical rotation becomes greater with increasing applied voltage. It is interesting to note that in the 2.5-kV case there is also a slight increase in the optical rotation outside the pretransitional region from the zero field results. Reproducibility of these measurements was always excellent. In Fig. 4, the curves seem to give the impression that the phase transition is shifting to higher temperatures with increasing field, but the following results show this to be incorrect. The magnitude of the fundamental frequency signal (corresponding to the optical rotation) was measured on cooling the mixture with a fixed voltage applied. Results of these measurements are given in Fig. 5; the oscillatory behavior

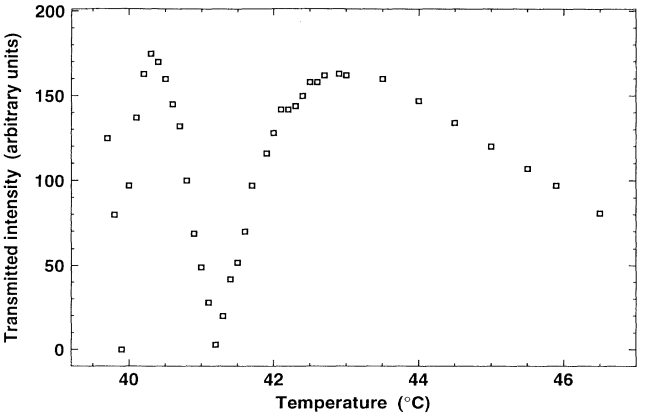

FIG. 5. Magnitude of the optical rotation signal measured by the lock-in amplifier on cooling mixture 34% (w/w) CE6–66% (w/w) CB5 with 2.5 kV applied.

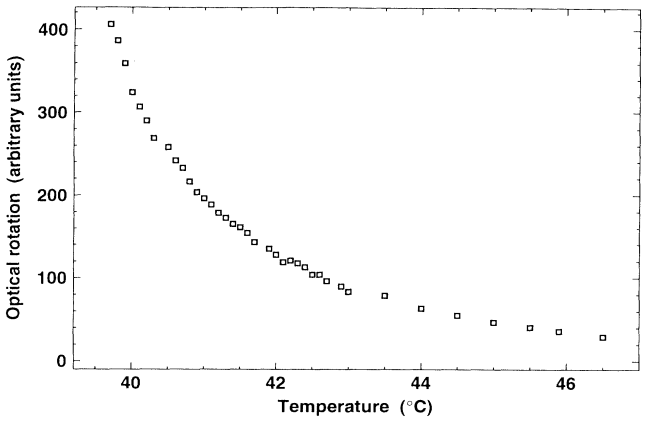

FIG. 6. Deconvoluted form of the curve in Fig. 5 (see text).

is due to the dependence of the transmitted intensity on $\sin 2(\phi+\theta)$ from Eq. (12). Accordingly, the optical rotation is proportional to $\sin^{-1}(I/I_{\max})$, where $I_{\max}$ is the maximum transmitted intensity in Fig. 5. The resultant deconvoluted curve is presented in Fig. 6 showing that the phase transition temperature is not shifting, but instead the optical rotation continues to increase sharply until the zero field isotropic-chiral nematic phase transition temperature of $\sim 40\,^{\circ}\mathrm{C}$ is reached. This was further verified by examining a 7.5-μm electro-optic cell containing the same mixture with comparable fields applied using polarizing microscopy. The appearance of chiral nematic droplets on cooling always occurred at the normal zero field phase transition temperature.

The field-induced experiment was repeated by replacing chiral CE6 with racemic CE6 at the same concentration of 34% (w/w). As expected, there was no consistent

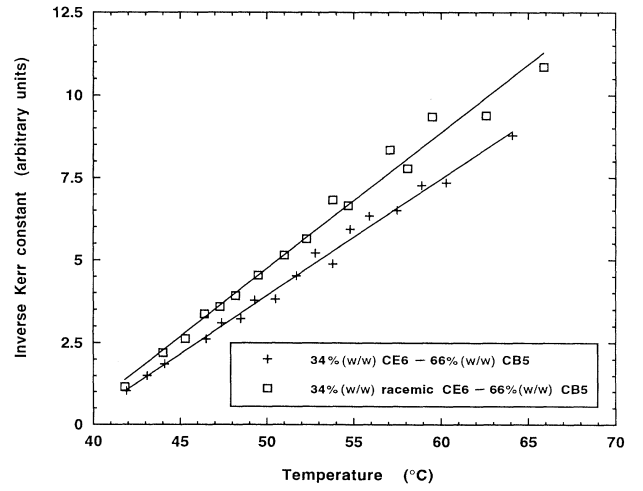

FIG. 7. Comparison of the pretransitional electric-field-induced birefringence effects in chiral and achiral mixtures of CE6–CB5; the ordinate is the inverse Kerr constant defined as $(\Delta n/\lambda E^2)^{-1}$, where Δn is the field-induced birefringence.

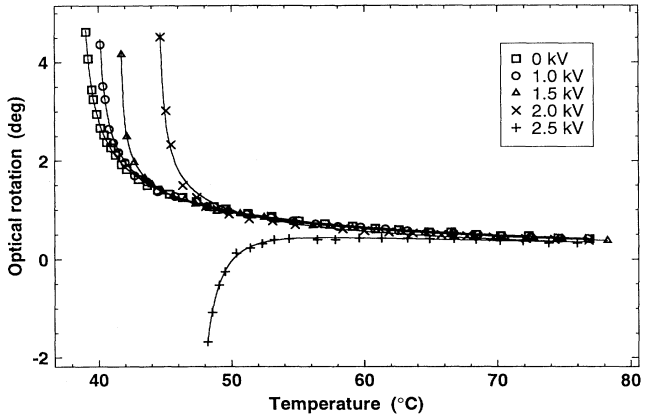

FIG. 8. Zero field and field-induced optical rotation in the isotropic phase as a function of temperature of mixture 14.1% (w/w) CE6–20.0% (w/w) racemic CE6–65.9% (w/w) CB5. The solid lines diverging positively are nonlinear least-squares fits to Eq. (16), i.e., $\phi=\phi_0+A/(T-T_1^*)^{1/2}$ and the solid line diverging negatively is the nonlinear least-squares fit to Eq. (18), i.e., $\phi=\phi_0+A/(T-T_1^*)^{1/2}-B/(T-T_2^*)^{1/2}$.

large increase of the signal in the pretransitional region. Although applied voltages of up to 3 kV were applied, only a small fluctuating signal was observed at the lock-in amplifier, which could not be nulled by rotating the analyzer.

Earlier, it was shown theoretically that the linear birefringence of a sample does not contribute to the optical rotation signal. One final check involved performing an experiment to measure the electric-field-induced birefringence as a function of temperature of both the chiral and achiral mixtures. The results for these mixtures are compared as linear plots of the inverse Kerr

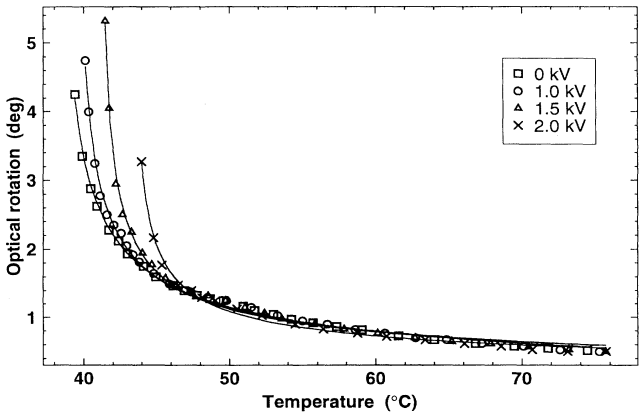

FIG. 9. Zero field and field-induced optical rotation in the isotropic phase as a function of temperature of mixture 17% (w/w) CE6–17% (w/w) racemic CE6–66% (w/w) CB5. The solid lines diverging positively are nonlinear least-squares fits to Eq. (16), i.e., $\phi=\phi_0+A/(T-T_1^*)^{1/2}$. In this case, the points corresponding to negative divergence were omitted.

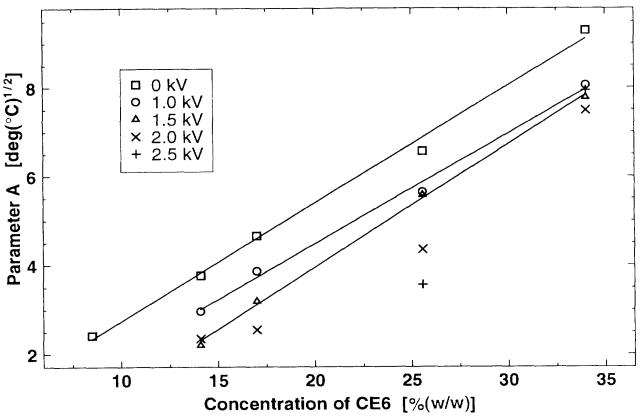

FIG. 10. Fitting parameter A as a function of CE6 concentration. The solid lines are linear least-squares fits.

constant against temperature in Fig. 7 and show that in the pretransitional region there is no significant difference in the field-induced birefringence for the chiral and achiral mixtures. This provides experimental evidence that the birefringence signal does not contribute to the optical rotation signal.

The effect of varying the chirality of the system was investigated by measuring the response of mixtures containing different amounts of racemic CE6 but maintaining the same overall composition of the CB5-CE6 mixture. Four other mixtures were prepared with concentrations of CE6 varying from 8.5% (w/w) to 25% (w/w). Figures 8 and 9 show the influence of applying voltages of up to 2.5 kV on the pretransitional optical activity of two of these mixtures. All field-induced experiments were performed using configuration 1 in Fig. 3. The field-induced behavior of the 25% (w/w) CE6–9% (w/w) racemic CE6–66% (w/w) CB5 mixture was similar but less pronounced than that of the initial mixture, i.e., 34% (w/w) CE6–66% (w/w) CB5. However, the field-induced

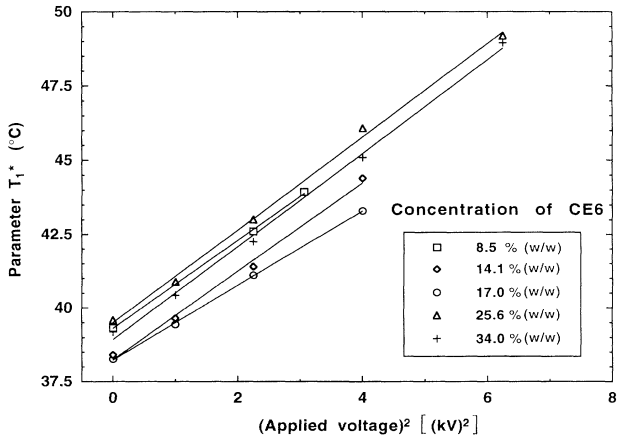

FIG. 11. Fitting parameter T_1^* as a function of the applied voltage squared. The solid lines are linear least-squares fits.

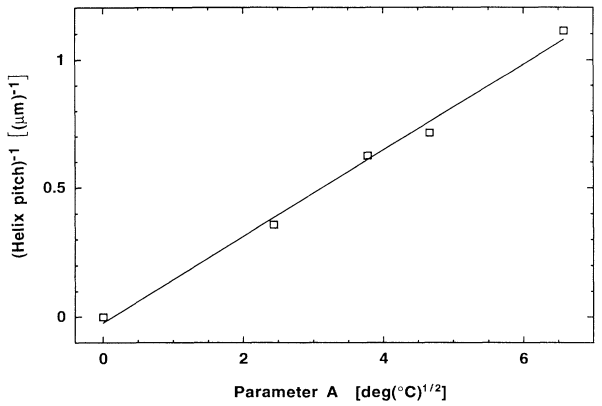

FIG. 12. The correlation between the inverse helix pitch and parameter A: results are for various CE6–racemic CE6–CB5 mixtures.

optical rotation became increasingly negative for mixtures of relatively low chirality [i.e., CE6 concentration $\leq 17\%$ (w/w)] and with large voltages applied (i.e., ≥ 1.5 kV). This anomalous behavior was not always reproducible exactly, as it is important to realize that the experimental conditions involved are critical in the pretransitional region. Electrohydrodynamic effects in the mixture had an adverse effect on the signal detected by the photodiode. In fact, conducting and nonconducting impurities lead to the instabilities that can mask the true field effects.

The positively diverging optical rotation data for all the mixtures was fitted to the simplified theoretical expression describing the optical rotation due to the molecular optical activity (2) and the conical spiral mode (8):

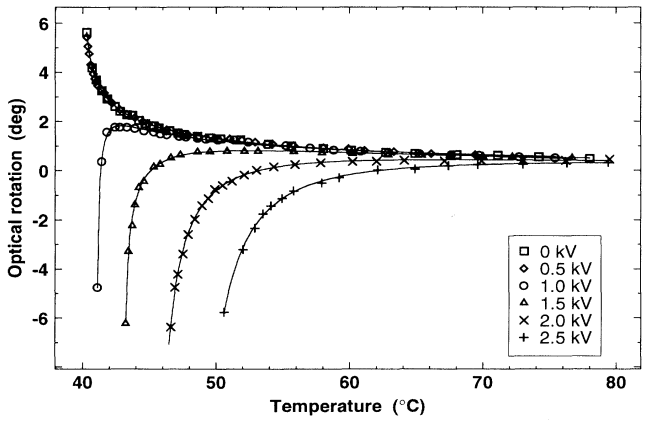

FIG. 13. Zero field and field-induced optical rotation in the isotropic phase as a function of temperature of a freshly prepared mixture of 17% (w/w) CE6–17% (w/w) racemic CE6–66% (w/w) CB5. The solid lines diverging positively are nonlinear least-squares fits to Eq. (16), i.e., $\phi=\phi_0+A/(T-T_1^*)^{1/2}$ and the solid lines diverging negatively are nonlinear least-squares fits to Eq. (18), i.e., $\phi=\phi_0+A/(T-T_1^*)^{1/2}-B/(T-T_2^*)^{1/2}$.

$$\phi=\phi_0+\frac{A}{(T-T_1^*)^{1/2}}\ , \tag{16}$$

where A is a fitting parameter. Agreement between experiment and theory was excellent. The positively diverging solid lines in Figs. 4, 8, and 9 represent the results of the three parameter nonlinear least-squares fits to (16). Parameters obtained from these fits were plotted as a function of concentration of CE6 and as a function of the applied voltage. In Fig. 10, parameter A seems to vary linearly with the concentration of CE6 as expected. The critical divergence temperature T_1^* was effectively independent of concentration and ϕ_0 was independent of field strength within experimental error. Increasing the electric field caused the amplitude A to decrease linearly with field strength, which may be a result of the electric field unwinding the local helix. Furthermore, in Fig. 11, the result that T_1^* increases as the square of the applied voltage can be anticipated from mean field theory [31]:

$$T^*=T_S^*(1+CE^2)\ , \tag{17}$$

where T_S^* is the susceptibility divergence temperature, C depends on the local electric susceptibility anisotropy, and E is the electric-field strength.

To relate the observed electro-chiral effects to chiral interactions, some measure of the chirality is required. As well as the optical activity, the helix pitch also provides information about the chiral strength of the mixtures studied. The helix pitch of these mixtures was measured using the Cano-wedge [32] technique, and verified using the diffraction [33] and spiral droplet [34] techniques. Figure 12 shows that the helix pitch is inversely proportional to the fitting parameter A determined from the zero field, optical rotation data fits.

Figure 13 shows the results of repeating the optical rotation measurements obtained in Fig. 9 but using a freshly prepared mixture of 17% (w/w) CE6–17% (w/w) racemic CE6–66% (w/w) CB5. Although the reproducibility is poor, the change in sign in the optical rotation on approaching the phase transition is indicative of mode coupling in highly chiral nematic liquid crystals. Hence we performed a five parameter nonlinear least-squares fit of all the anomalous experimental data to a simplified version of the full expression in (1), which includes the contribution from the planar spiral mode:

$$\phi=\phi_0+\frac{A}{(T-T_1^*)^{1/2}}-\frac{B}{(T-T_2^*)^{1/2}}\ , \tag{18}$$

where the fitting parameters are A, B, T_1^*, T_2^*, and ϕ_0. The fits were generally excellent and it seems there is a theoretical basis for our observations since Eq. (18) based on this theory can be fitted to the observed results with a high degree of precision. From the data fits of the mixture in Fig. 13, B was found to change significantly with increasing field. We tentatively attribute this behavior to a change in induced order due to the electric field, resulting in possible field-induced coupling between the conical and planar spiral modes.

CONCLUSION

In this paper, we have reported results of field-induced optical rotation in the pretransitional isotropic region of chiral nematic mixtures that have a strong positive dielectric anisotropy. We have shown that this induced optical rotation can diverge in the positive or negative direction depending on the chiral strength of the mixtures and the magnitude of the electric field applied. Furthermore, the behavior of the field-induced optical activity in the pretransitional isotropic region was modeled excellently by theoretical expressions based on a Landau–de Gennes approach that describes natural pretransitional optical activity phenomena. Field effects on chiral fluctuations provide a new probe of chiral interactions, and measurements in the pretransitional region of smectic C^*, TGBA*, TGBC*, and other helicoidal liquid crystal phases should give more detailed information on the local molecular interactions responsible for these phases.

ACKNOWLEDGMENTS

The authors would like to thank the UK Science and Engineering Research Council (SERC) and Defence Research Agency (DRA) for financial support as well as Merck Ltd. for provision of materials CE6, racemic CE6, and CB5.

[1] P. G. de Gennes, Phys. Lett. A **30**, 454 (1969).
[2] P. G. de Gennes, Mol. Cryst. Liq. Cryst. **12**, 193 (1971).
[3] J. Cheng and R. B. Meyer, Phys. Rev. Lett. **29**, 1240 (1972).
[4] J. Cheng and R. B. Meyer, Phys. Rev. A **9**, 2744 (1974).
[5] H. R. Trebin Phys. Bl. **44**, 221 (1988).
[6] S. A. Brazovskii and S. G. Dmitriev, Zh. Eksp. Teor. Fiz. **69**, 979 (1975) [Sov. Phys. JETP **42**, 497 (1976)].
[7] P. P. Crooker, Liq. Cryst. **5**, 751 (1989).
[8] D. C. Wright and N. D. Mermin, Rev. Mod. Phys. **61**, 385 (1989).
[9] E. J. Demikhov and V. K. Dolganov, Pis'ma Zh. Eksp. Teor. **38**, 368 (1983) [JETP Lett. **38**, 445 (1984)].
[10] V. M. Filev, Pis'ma Zh. Eksp. Teor. Fiz. **37**, 589 (1983) [JETP Lett. **37**, 703 (1983)].
[11] J. E. Wyse and P. J. Collings, Phys. Rev. A **45**, 2449 (1992).
[12] P. R. Battle, J. D. Miller, and P. J. Collings, Phys. Rev. A **36**, 369 (1987).
[13] R. Parthasarathy and D. B. Dupre, Liq. Cryst. **3**, 1231 (1988).
[14] J. E. Wyse, J. Ennis, and P. J. Collings, Phys. Rev. Lett. **62**, 1045 (1989).
[15] F. Vanweert, W. Demol, and W. Van Dael, Liq. Cryst. **5**, 853 (1989).
[16] V. A. Kizel and S. I. Panin, Zh. Eksp. Teor. Fiz. **93**, 186 (1987) [Sov. Phys. JETP **66**, 105 (1987)].
[17] E. Demikhov, J. Hollmann, and P. Pollmann, Europhys. Lett. **21**, 581 (1993).
[18] E. Voss, P. Pollmann, and J. Hollmann, Ber. Bunsenges. Phys. Chem. **97**, 1205 (1993).
[19] P. J. Collings, Mod. Phys. Lett. B **6**, 425 (1992).
[20] J. W. Goodby, Liq. Cryst. **14**, 37 (1993).
[21] V. N. Tsvetkov and E. I. Ryumstev, Kristallografiya **13**, 290 (1968) [Sov. Phys. Cryst. **13**, 225 (1968)].
[22] D. A. Dunmur and A. E. Tomes, Mol. Cryst. Liq. Cryst. **76**, 231 (1981).
[23] W. Pyzuk, I. Slomka, J. Chrapec, S. Rzoska, and J. Ziolo, Chem. Phys. **121**, 255 (1988).
[24] L. J. Martinez-Miranda, R. Kawakami, N. Engheta, and K. B. O'Brien, Liq. Cryst. **14**, 1439 (1993).
[25] E. Charney, *The Molecular Basis of Optical Activity: Optical Rotary Dispersion and Circular Dichroism* (Wiley, New York, 1979).
[26] D. Bensimon, E. Domany, and S. Shtrikman, Phys. Rev. A **28**, 427 (1983).
[27] V. K. Dolganov, S. P. Krylova, and V. M. Filev, Zh. Eksp. Teor. Fiz. **78**, 2343 (1980) [Sov. Phys. JETP **51**, 1177 (1980)].
[28] R. M. Hornreich and S. Shtrikman, Phys. Rev. A **24**, 635 (1981).
[29] K. C. Frame, J. L. Walker, and P. J. Collings, Mol. Cryst. Liq. Cryst. **198**, 91 (1991).
[30] E. I. Demikhov, V. K. Dolganov, and V. M. Filev, Pis'ma Zh. Eksp. Teor. Fiz. **37**, 305 (1983) [JETP Lett. **37**, 361 (1983)].
[31] P. Palffy-Muhoray and D. A. Dunmur, Mol. Cryst. Liq. Cryst. **97**, 337 (1983).
[32] R. Cano and P. Chatelain, C. R. Acad. Sci. **253**, 208 (1961).
[33] C. M. Waters, F. C. Saunders, and M. G. Clark, Mol. Cryst. Liq. Cryst. **46**, 261 (1981).
[34] S. Candau, P. Le Roy, and F. Debeauvais, Mol. Cryst. Liq. Cryst. **23**, 283 (1973).